Research Article

# Preparation, Characterization and *In-Vitro* Anti-Inflammatory Activity of Gold Nanoparticles from *Moullava spicata* Dalzell Leaf

**Asha Golasangimath[1], Rajesh Shastry[2], Prasanna Habbu[3], Sudhir Iliger[4], V.H. Kulkarni[5]**

1. Department of Pharmacognosy, SET's College of Pharmacy, Dharwad, Karnataka, India.
2. Associate Professor Department of Pharmacognosy, SET's College of Pharmacy, Dharwad, Karnataka, India.
3. Head Department of Pharmacognosy, SET's College of Pharmacy, Dharwad, Karnataka, India.
4. Head Department of Pharmaceutics, SET's College of Pharmacy, Dharwad, Karnataka, India.
5. Principal Department of Pharmacology, SET's College of Pharmacy, Dharwad, Karnataka, India.

***Corresponding author's E-mail:** ashagolasangimath1996@gmail.com

**Received:** 12-10-2025; **Revised:** 25-11-2025; **Accepted:** 02-12-2025; **Published online:** 20-12-2025.

**ABSTRACT**

The expanding field of nanotechnology has opened new possibilities in biomedical science, particularly for therapeutic delivery and disease management. Gold nanoparticles (AuNPs) have gained special attention due to their favorable stability, biological compatibility and adjustable characteristics. To avoid the environmental concerns associated with chemical synthesis, the present study employed a plant-based method to prepare AuNPs using the leaf extract of *Moullava spicata* Dalzell. Fresh leaves were authenticated, processed into powder and examined for their physicochemical and phytochemical composition. The aqueous extract, which contained abundant phenolic and flavonoid compounds, acted as both reducing and stabilizing medium for converting $HAuCl_4$ into MS-GNPs. Formation of nanoparticles was evident through a distinct color change from bluish gray to purple and an absorption peak corresponding to surface plasmon resonance at 533-538 nm. FTIR analysis suggested that functional groups such as hydroxyl, amine and carbonyl units are present in MSGNPs. X-ray diffraction confirmed a crystalline structure with a FCC arrangement, while TEM images revealed spherical particles with an average diameter of about 53.6 nm. DLS and zeta potential measurements (–14.8 mV) indicated moderate stability of the colloidal suspension. The synthesized nanoparticles showed marked anti-inflammatory activity, including an 87% inhibition of protein denaturation at 200 µg/mL and noticeable suppression of MMP-2 and MMP-9 activity in gelatin zymography, showing performance comparable to reference drugs. These findings demonstrate that *Moullava spicata* leaf extract provides an efficient green route for AuNP synthesis and yields nanoparticles with significant anti-inflammatory potential. Further *in-vivo* investigations are encouraged to explore their therapeutic applicability.

**Keywords:** *Moullava spicata*, Gold nanoparticles, Green synthesis, Anti-inflammatory activity, Protein denaturation assay, Gelatin zymography.

## INTRODUCTION

Inflammation is a complex protective response of vascular tissues that becomes activated when the body encounters infection, physical injury or chemical irritation and persistent inflammation contributes to several chronic diseases[1]. Although synthetic anti-inflammatory drugs are widely used, prolonged therapy often leads to adverse effects, creating the need for safer alternatives[2].

Nanotechnology offers new opportunities in biomedical applications, particularly through the use of gold nanoparticles (AuNPs), which are valued for their biocompatibility and tunable physicochemical features[3]. Green synthesis of AuNPs using plant extracts has emerged as an eco-safe method that avoids toxic chemicals, as phytochemicals act as natural reducing and stabilizing agents[4].

*Moullava spicata* Dalzell is a medicinal plant rich in flavonoids, tannins, alkaloids and phenolic compounds, many of which exhibit antioxidant and anti-inflammatory properties[5]. Previous research on plant-based AuNPs has demonstrated enhanced biological activities, including strong anti-inflammatory effects[6]. Plants with high antioxidant potential are especially suitable for nanoparticle synthesis because their phytochemicals efficiently support reduction and stabilization[5].

Although various plant extracts have been used to generate AuNPs with therapeutic potential, the application of *Moullava spicata* in nanoparticle synthesis remains largely unexplored. Studies from last few year highlights that green-synthesized AuNPs can suppress inflammatory marker, improve stability and enhance delivery efficiency, making them ideal for biomedical use[6].

Therefore, the present study aims to synthesize gold nanoparticles using *Moullava spicata* leaf extract via a green approach, characterize the nanoparticles using standard analytical methods and to evaluate their *in-vitro* anti-inflammatory activity.

## MATERIALS AND METHODS

### MATERIALS

Analytical grade chemicals were used for all experiments. Ethanol, $AlCl_2$, sodium carbonate potassium acetate etc. were obtained from S.D. Fine-Chem Ltd., Mumbai. Quercetin and Gallic acid standards were sourced from Sigma-Aldrich, Mumbai and Chloroauric acid ($HAuCl_4$) from

Oxford Lab Fine Chem LLP, Maharashtra. Bovine serum albumin, sodium chloride and potassium chloride were purchased from Loba Chemie Pvt. Ltd. Buffer salts-monopotassium phosphate and disodium phosphate were procured from Hi-Media Laboratories Pvt. Ltd., Mumbai and diclofenac sodium from Dr. Reddy's Laboratories.

**Collection and authentication of plant material**

Fresh leaves of *Moullava spicata* Dalzell (Fabaceae) were collected in June 2025 from the semi- evergreen regions of the Kumbarwada Forest Range, Central Western Ghats, Uttara Kannada District, Karnataka, India. The plant was authenticated by Dr. Harsha Hegde, Scientist-E, ICMR–National Institute of Traditional Medicine, Belagavi. A voucher specimen (Accession No.: SETCPD/Ph.cog/herb/01/2025) was deposited in the Department of Pharmacognosy, SET's College of Pharmacy, Dharwad.

## METHODS

***Pharmacognostical Evaluation***

**Morphological and organoleptic characteristics**

Macroscopic and sensory characteristics of the leaves—such as color, odor, taste, size, texture and shape—were assessed according to standard pharmacognostic procedures described by Evans[7] and Iyengar[8].

**Proximate analysis**

Quality-control parameters, including moisture content, extractive values (water-soluble and alcohol-soluble) and ash values (total, acid-insoluble, water-soluble and sulphated), were determined following the guidelines of the World Health Organization[9] and the Ayurvedic Pharmacopoeia of India[10].

***Preparation of extracts***

Fresh leaves were washed thoroughly, rinsed with distilled water and shade-dried for 10-15 days. The dried leaves were pulverized and stored in airtight containers.

**Aqueous Extract (MSA-I):**

Powdered leaf material (100 g) was macerated with 1000 mL chloroform water I.P. (1:10 w/v) for 72 h at room temperature with intermittent shaking. The extract was filtered, concentrated using a rotary evaporator at 40 °C, dried and stored in a desiccator over anhydrous calcium chloride. The percentage yield was recorded.

**Alcoholic Extract (MSE-I)**

Similarly, 100 g of leaf powder was macerated with 1000 mL of 95% ethanol in an amber- colored flask for 72 h with occasional shaking. The extract was filtered, concentrated under reduced pressure, dried and stored in a vacuum desiccator. The percentage yield was recorded.

## PHYTOCHEMICAL INVESTIGATION

Preliminary phytochemical testing of aqueous and alcoholic extracts was carried out using conventional qualitative procedures described by K.R. Khandelwal[11] and C.K. Kokate[12].

## QUANTITATIVE DETERMINATION OF SECONDARY METABOLITES[13]

Phenolic and flavonoid constituents-major contributors to antioxidant and anti-inflammatory activity were quantitatively assessed.

**Estimation of Total Phenolic Content (TPC)**

One gram of extract was subjected to methanolic maceration and the Folin-Ciocalteu method was used to determine TPC. Absorbance was measured at 765 nm and results were expressed as mg of gallic acid equivalents (GAE)/g extract.

**Estimation of Total Flavonoid Content (TFC)**

Flavonoid content was measured using the Aluminium-Chloride colorimetric method. Absorbance was recorded at 415 nm and TFC was expressed as mg of quercetin equivalents (QE)/g extract.

## GREEN SYNTHESIS OF METAL-BASED NANOPARTICLES[14]

**Preparation of precursor solution**

A 1 mM chloroauric acid ($HAuCl_4$) solution was freshly prepared and used as the metallic precursor for gold nanoparticle synthesis

**Plant-mediated synthesis of gold nanoparticles**

Gold nanoparticles (AuNPs) were produced by combining 3 mL of the aqueous leaf extract with 7 mL of 1 mM $HAuCl_4$. The reaction mixture was kept under ambient light at room temperature for 24 hours. The characteristic color transition from bluish-gray to purple indicated the nanoparticle formation. The reaction mixture was centrifuged at 10,000 rpm for 30 minutes and the resulting pellet was washed several times with distilled water to remove unbound residues. The purified AuNPs were dried and stored at 4 °C until further evaluation.

## CHARACTERIZATION OF SYNTHESIZED GOLD NANOPARTICLES[15-17]

**UV-VIS Spectroscopy**

Formation of MSGNPs was confirmed by recording the absorption spectrum between 450-650 nm using a quartz cuvette with distilled water serving as the blank.

**FTIR Analysis**

The functional groups present in the nanoparticles were identified using the KBr pellet method. MSGNPs were harvested after 4 hours of incubation through centrifugation, dried and then subjected to FTIR analysis.

**Particle Size Analysis**

Dynamic light scattering was performed using a HORIBA SZ-100 Analyzer (90° angle, 25 °C) to determine mean particle size, Z-average and PDI of the synthesized nanoparticles.

**X-Ray Diffraction (XRD)**

Crystalline nature of the MSGNPs was analyzed using an XRD instrument equipped with Cu Kα radiation operated at 40 kV and 20 mA. The average crystallite size was calculated using the Debye-Scherrer equation.

**Zeta Potential Analysis**

Zeta potential was measured using a HORIBA SZ-100 Analyzer under standard electrophoretic light-scattering conditions after dilution in $2 \times 10^{-2}$ M NaCl.

**Transmission Electron Microscopy (TEM) with Energy Dispersive Spectroscopy (EDS)**

TEM and EDS were performed using OXFORD instruments. A drop (5-10 µL) of the nanoparticle suspension was deposited onto a carbon-coated copper grid and allowed to air-dry. TEM imaging was performed at an operating voltage of 2-3 kV to visualize morphology, while EDS spectra were recorded to confirm the elemental composition of the synthesized gold nanoparticles.

**IN-VITRO ANTI-INFLAMMATORY ACTIVITY**

**Detection of MMP-2 and MMP-9 by gelatin zymography**[18,19]

Matrix metalloproteinase (MMP-2 and MMP-9) were analyzed using gelatin zymography. A 10% resolving gel and 5% stacking gel were prepared and electrophoresis was carried out at 80 V until the dye front reached the bottom. Gels were washed with 2.5% Triton X-100, incubated overnight at 37 °C, stained with 0.5% Coomassie Blue R-250 and destained to visualize clear bands indicating enzyme activity. Band intensities MMP-2 (gelatinase A, ~72 kDa) and MMP-9 (gelatinase B, ~95 kDa) were analyzed using Total Lab Software (UK).

**Protein Denaturation Assay**[20,21]

Anti-inflammatory activity was evaluated using the protein denaturation method. Reaction mixtures containing 3% BSA solution and test samples (100-1000 µg/ml) were incubated at 37°C for 20 min, followed by adding PBS solution and heating at 80 °C for 10-20 min. After cooling, absorbance was measured at 660 nm. Diclofenac sodium served as the standard and distilled water as control. The percentage inhibition of protein denaturation was calculated by using formula:

$$\% \text{ Inhibition} = \frac{\text{A control} - \text{A sample}}{\text{A control}} X100$$

Where: *A control* = Absorbance of control and *A sample* = Absorbance of test or standard.

## RESULTS AND DISCUSSION

### RESULTS

**Pharmacognostical Evaluation:**

**Organoleptic Study:**

The leaves of *Moullava spicata* were found to be bipinnate with oblong, coriaceous leaflets measuring approximately 3-5 cm in length. The upper surface of leaf appeared dark green and slightly glossy, whereas the lower surface was light green. The texture was leathery with a fibrous fracture. The leaves were odorless and exhibited bitter taste. A notable identifying feature was the presence of small, sharp prickles along the rachis which is the characteristic of *Moullava* genus. The photographs of plant's climbing habit and leaves are shown in Figure 1.

**Figure 1:** Photographs showing the Climbing habit and leaves of *Moullava spicata* Dalzell Physico-chemical studies

The proximate evaluation of the leaf powder of *Moullava spicata* showed moisture content of 7.5%. The extractive values indicated higher solubility in water (27.5%) compared to alcohol (24.5%). Ash analysis revealed a total ash value of 5.1% with 2.0% acid-insoluble ash, 1.0% water-soluble ash and 2.5% sulphated ash.

**Preliminary Qualitative Phytochemical Analysis**

Preliminary phytochemical screening of aqueous and ethanolic leaf extract was performed using standard methods to identify the presence of major phytoconstituents, including carbohydrates, proteins and amino acids, alkaloids, flavonoids, glycosides (saponin /cardioactive), tannins and phenolics, steroids/ terpenoids and coumarins.

$$\text{Extractive value } (\%\frac{w}{w}) = \frac{\text{Weight of dried extract}}{\text{Weight of plant powder taken}} \times 100$$

The aqueous extract (MSA-1) appeared reddish-brown in color with a characteristic odor and showed a crystalline consistency. From 10 g of powdered leaf material, 2.75 g of dried extract was obtained, corresponding to a yield of 27.50% (w/w). The ethanolic extract (MSE-1) was dark

brown with a characteristic odor and exhibited a hard solid consistency. From the same initial quantity of plant powder (10 g), 2.45 g of dried extract was recovered, giving a yield of 24.50% (w/w).

**Preliminary phytochemical analysis of aqueous and ethanolic leaf extracts of *Moullava spicata*.**

Phytochemical analysis of the aqueous (MSA-I) and ethanol (MSE-I) extracts of *Moullava spicata* revealed the presence of several primary and secondary metabolites. The aqueous extract confirmed the presence of tannins, phenolic compounds and flavonoids, while carbohydrates, cardiac glycosides, proteins and amino acids were moderately present. Alkaloids and saponins were detected in trace amounts. In comparison, the ethanol extract exhibited moderate levels of tannins, phenolic compounds and alkaloids with weak reactions for carbohydrates, flavonoids and cardiac glycosides.

**Quantitative Determination of Secondary Metabolites**

**Estimation of Total Flavonoid and Phenolic Content**

The total flavonoid content was estimated by the aluminum chloride colorimetric method using quercetin as the standard. The extract contained 38.80 mg QE/g of dried extract. The total phenolic content was determined using the Folin–Ciocalteu method with gallic acid as the reference standard. The extract contained 50.90 mg GAE/g of dried extract. The calibration curves for standard Quercetin and Gallic acid are presented in Figure 2.

**Synthesis and Characterization of Gold Nanoparticles**

In the current study, the primary phytochemical components present in the aqueous leaf extract of *M. spicata* were identified. According to literature reports, aqueous extracts are commonly utilized for the green synthesis of gold nanoparticles (AuNPs). Hence, both ethanolic and aqueous extracts were evaluated for their potential to act as reducing and stabilizing agents in the bioreduction of gold ions ($Au^{3+}$) from chloroauric acid ($HAuCl_4$) to elemental gold. Although both extracts facilitated nanoparticle formation, the aqueous extract yielded a higher concentration of nanoparticles and also demonstrated superior response in total phenolic content (TPC) and total flavonoid content (TFC) assays compared to the ethanolic extract. Hence, the aqueous extract was selected for further synthesis. The reaction mixture was incubated under both light and dark conditions for 24 h. It was observed that exposure to light enhanced nanoparticle formation, whereas dark conditions produced a relatively lower yield. The formation of gold nanoparticles was confirmed visually by a noticeable color transition of the solution from bluish-grey to purple which is shown in Figure 3.

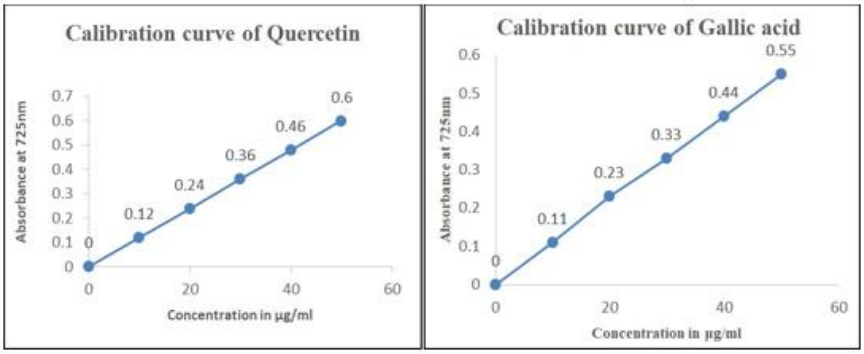


**Figure 2:** Standard calibration curve of Quercetin and Gallic acid for estimation of total flavonoid and phenolic content


**Figure 3:** Green synthesis of *Moullava spicata*-mediated gold nanoparticles (MSGNPs).

Figure 3 showing colour change from bluish-grey to purple, for different concentrations confirming formation of AuNPs.

**Characterization of Gold Nanoparticles**

The biosynthesized nanoparticles were characterized using UV-Vis Spectroscopy, TEM-EDX (CFC-SAIF-DST Centre Shivaji University, Kolhapur), X-Ray Diffraction, Zeta Potential, FTIR and Dynamic Light Scattering (DLS) to determine their optical properties, morphology, size distribution, crystalline structure, surface charge and functional groups involved in stabilization.

**UV-Vis Spectroscopy :**

The formation of gold nanoparticles was confirmed using

UV-Vis spectroscopy by detecting surface plasmon resonance (SPR). In this study, as shown in figure 4, the *M. spicata* extract combined with $HAuCl_4$ showed a prominent absorption peak at 533-538 nm, which is indicative of AuNPs. The presence of a narrow peak in this range confirms the successful reduction of $Au^{3+}$ ions to $Au^0$ elements.

**Fourier Transform Infrared Spectroscopy (FTIR)**

The FTIR spectrum identified the functional groups present in MSGNPs. As shown in figure 4 the prominent peaks at 3896–3752 $cm^{-1}$, 3400 $cm^{-1}$ and 3178 $cm^{-1}$ indicated the presence ofhydroxyl and amine groups. Peaks at 1675 and 1607 $cm^{-1}$ corresponded to phenolics, flavonoids and proteins, while signals at 845 and 747 $cm^{-1}$ confirmed aromatic compounds. Additionally, a band at 584 $cm^{-1}$ suggested metal-oxygen interactions, indicating the binding of gold with plant-derived phytochemicals.

**Transmission Electron Microscopy and Energy Dispersive X-Ray (TEM-EDX):**

TEM micrographs shown in Figure 5-I (a–f) revealed that the AuNPs were predominantly spherical, with an average size of 53.6 ±6.8 nm (N = 17), within the range of 40-67 nm. Particles were well distributed. High-resolution TEM showed clear lattice fringes, while SAED patterns confirmed the Face Centered Cubic (FCC) crystalline structure of gold.

EDS elemental mapping shown in Figure 5-II confirmed gold (Au, yellow) as the major element. Carbon (C, green) signals originated from phytochemicals in the extract, while minor copper (Cu, red) signals arose from the TEM grid. The EDS spectrum as shown in Figure 5-III displayed strong peaks for Au at 2-3 keV, confirming nanoparticle composition. Quantitative analysis showed 93.13% Au and 6.87% C by weight, further validating nanoparticle purity and organic stabilization.

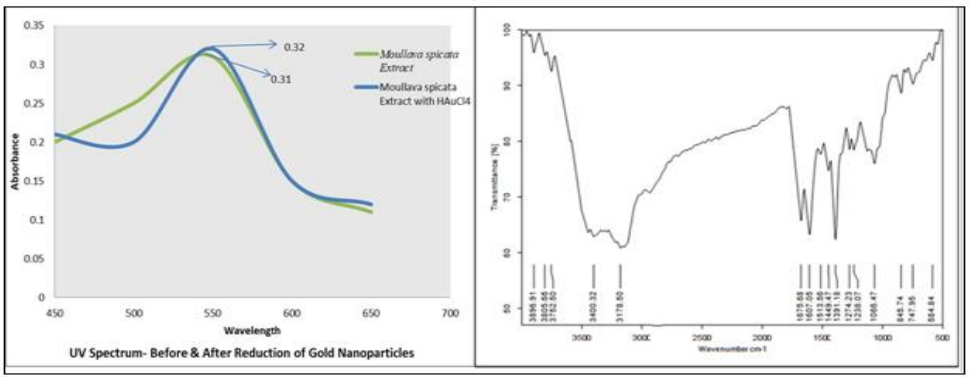


**Figure 4:** UV Spectrum and FTIR spectrum of *Moullava spicata* Gold Nanoparticles

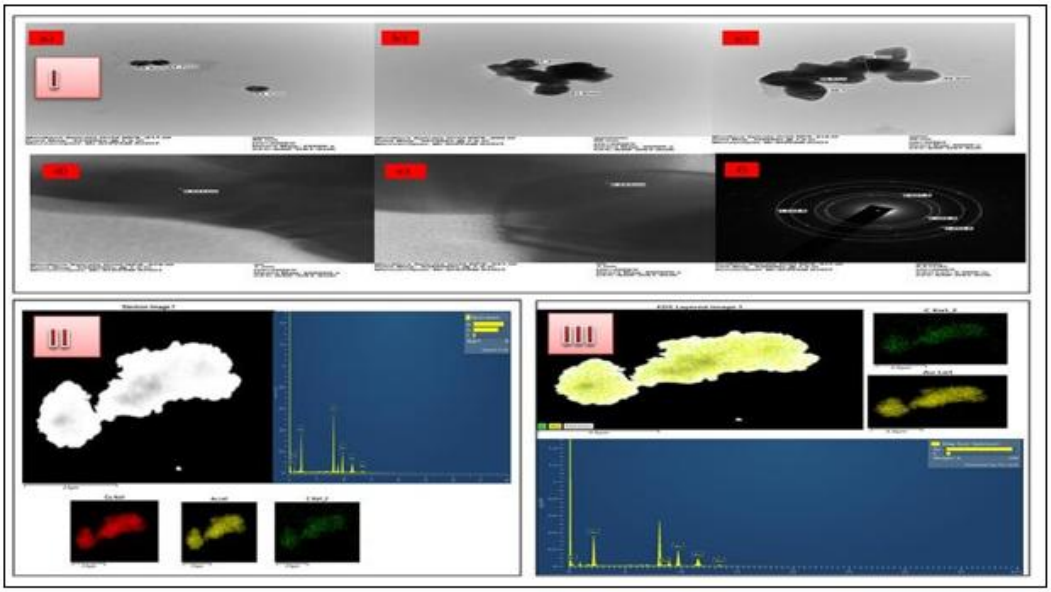

**Figure 5:**

**I.** TEM micrographs of *M. spicata*-mediated AuNPs showing (a-c) spherical nanoparticles with sizes of 40-67 nm, HRTEM (d-e) images displaying lattice fringes and SAED (f) pattern confirming the crystalline FCC structure of gold.

**II.** EDS elemental mapping of MSGNPs showing Au (yellow) as the major component, C (green) from phytochemicals, and Cu (red) from the supporting grid.

**III.** TEM-EDS spectrum of *Moullava spicata*-mediated AuNPs showing strong Au and C peak from plant phytochemicals.

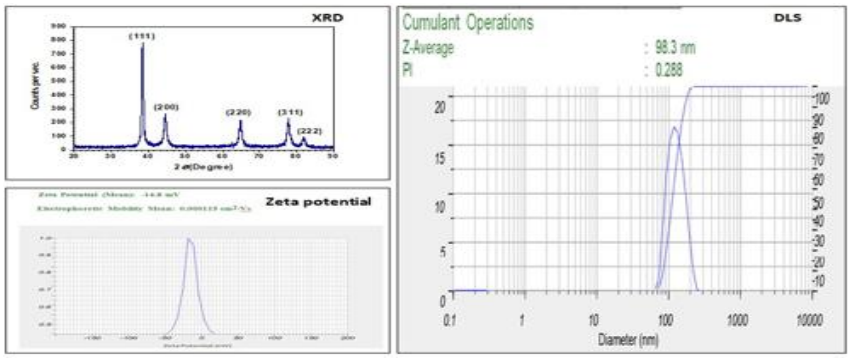


**Figure 6:** XRD, Zeta potential and dynamic light scattering Analysis of MSGNPs

**X-Ray Diffraction (XRD)**

The XRD pattern as shown in Figure 6, It showed intense diffraction peaks at (111), (200), (220), (311) and (222) planes, consistent with the FCC crystalline structure of Au (JCPDS No. 00-066- 0091). The dominance of the (111) plane indicates preferred orientation of crystal growth.

**Zeta Potential Analysis**

Zeta potential analysis as shown in Figure 6, revealed a surface potential of -14.8 mV with electrophoretic mobility of –0.000115 $cm^2/V{\cdot}s$. The negative charge indicates capping by anionic phytochemicals from the extract, imparting moderate colloidal stability to the nanoparticles.

**Dynamic Light Scattering (DLS) Analysis**

The average particle size (Z-average) determined by DLS was 98.3 nm as shown in Figure 6, with a polydispersity index (PDI) of 0.288, indicating a relatively narrow size distribution and good homogeneity. The results confirm the nanoparticles were within the nanometer range and moderately monodisperse.

***IN-VITRO* ANTI-INFLAMMATORY ACTIVITY**

The anti-inflammatory activity of MS-GNPs was evaluated using gelatin zymography and protein denaturation assay at different concentrations.

**Gelatin Zymography: Detecting MMP-9 and MMP-2**

The results of gelatin zymography were presented in Table 1, Figure 7. Following electrophoresis and Coomassie blue staining, translucent white bands on a dark blue background indicated regions of gelatin degradation. The uniformly blue-stained gel background represents intact gelatin, while the white bands correspond to gelatinase.

- The lower band was identified as gelatinase A(MMP-2, ~72kDa)
- The upper band was identified as gelatinase B (MMP-9, ~95kDa)

The test sample (MS-GNPs) demonstrated significant inhibition of gelatinase activity compared with the negative control. Quantitative band intensity analysis showed 56% inhibition of MMP- 2 and 49% inhibition of MMP-9. In contrast, the positive control (tetracycline HCl) exhibited complete inhibition (100%) of both enzymes. These results confirm that MS-GNPs were capable of suppressing gelatinase enzymes involved in inflammatory pathways, highlighting their potential as anti-inflammatory agents.

**Protein Denaturation Assay**

The protein denaturation assay (Figures 7) was carried out to evaluate the anti-inflammatory potential of MS-GNPs. The assay relies on the inhibition of heat-induced denaturation of bovine serum albumin (BSA). Different concentrations of MS-GNPs (100-1000 µg/ml) were tested and compared with Diclofenac sodium (standard drug) and distilled water (control). Absorbance values were recorded at 660 nm and percentage inhibition was calculated using the formula:

$$\% \text{ Inhibition} = \frac{\textbf{Abs of Control} - \textbf{Abs of Sample}}{\textbf{Abs of Control}} \boldsymbol{X\ 100}$$

MS-GNPs exhibited concentration-dependent inhibition of protein denaturation. The inhibition ranged from 62% to 87%, with maximum inhibition at 200 µg/ml (87%). At higher concentrations (400-1000 µg/ml), moderate inhibition was observed (71%, 65% and 62% respectively). Diclofenac sodium exhibited maximum inhibition (90%), while the control showed no inhibition. These findings suggest that MS-GNPs possess significant anti-inflammatory activity, comparable to the standard drug and have the ability to stabilize proteins against denaturation.

**Table 1:** Inhibition of MMP-2 and MMP-9 by MS-GNP and controls

| Sl.No. | NAME OF THE COMPOUND | % BANDS OF MMP | | % INHIBITION OF MMP | |
|---|---|---|---|---|---|
| | | MMP 2 | MMP 9 | MMP 2 | MMP 9 |
| 1 | Negative Control (Supernatant of Squamous cell carcinoma) | 100 | 100 | 0 | 0 |
| 2 | Positive Control (Tetracycline HCL) | 0 | 0 | 100 | 100 |
| 3 | Test sample (MS-GNP) | 44 | 51 | 56 | 49 |

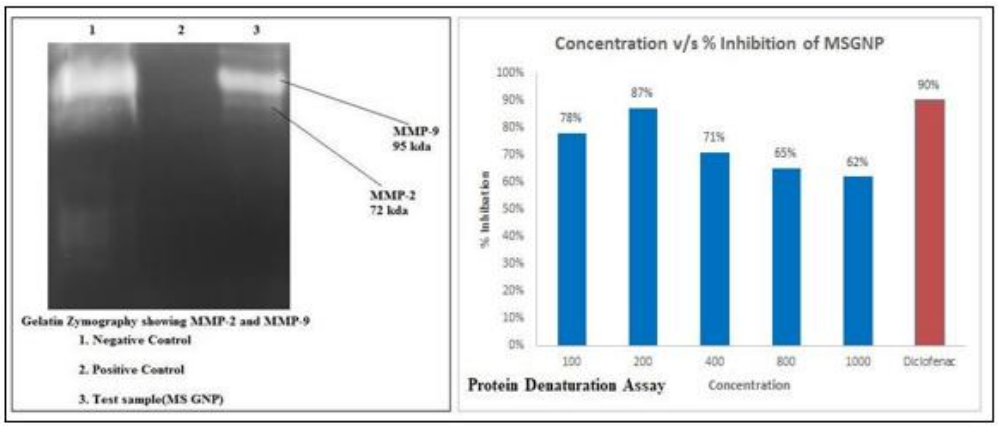


**Figure 7:** Gelatin Zymography and Protein Denaturation Assay showing anti-inflammatory activity of MSGNPs compared with Tetracycline HCl and Diclofenac sodium respectively**.**

## DISCUSSION

Green synthesis of nanoparticles using plant extracts has emerged as an environmentally safe and cost-effective approach compared with conventional methods. Gold nanoparticles (AuNPs) are widely studied due to their stability, surface plasmon resonance (SPR) and biomedical applications. In the present work, AuNPs were synthesized using the aqueous extract of *Moullava spicata* and the characteristic color change to purple confirmed nanoparticle formation, consistent with previous reports on green-synthesized AuNPs[22].

Both aqueous and alcoholic extracts facilitated reduction of $Au^{3+}$ ions; however, the aqueous extract produced a higher yield, possibly due to the better solubility of polar phytochemicals such as phenolics, flavonoids and tannins that act as reducing and stabilizing agents[23]. Light exposure further improved synthesis efficiency, likely due to photoreduction-mediated acceleration of electron transfer, which has also been reported in earlier studies[24].

Phytochemical analysis revealed the presence of flavonoids, tannins, alkaloids and phenolics, which are known to participate in metal ion reduction and nanoparticle stabilization. The high phenolic and flavonoid content supports the better anti-inflammatory potential of the extract.

Characterization confirmed the formation of stable AuNPs. UV–Vis spectroscopy showed a distinct SPR band, TEM revealed predominantly spherical nanoparticles and XRD confirmed crystalline nature. FTIR identified functional groups present in MSGNPs, while DLS and zeta potential indicated moderate stability and good dispersion uniformity.

The nanoparticles demonstrated notable anti-inflammatory activity. Gelatin zymography showed inhibition of MMP-2 and MMP-9, indicating the potential of MS-GNPs to modulate extracellular matrix degradation[25]. Protein denaturation assays showed concentration- dependent inhibition comparable to diclofenac sodium, although slight reduction at higher concentrations may be due to nanoparticle aggregation[26].

Overall, the study demonstrates that *Moullava spicata* extract effectively facilitates the green synthesis of AuNPs and contributes to their biological activity. These findings support the potential of MS-GNPs as a natural, eco-friendly and biocompatible anti-inflammatory agent.

## CONCLUSION

*Moullava spicata*-mediated gold nanoparticles (MS-GNPs) demonstrated significant *in-vitro* anti-inflammatory activity, with 87% inhibition of protein denaturation and effective suppression of MMP-2 and MMP-9 activities. These findings highlight their potential as natural, biocompatible alternatives to conventional anti-inflammatory drugs. Further studies were recommended to isolate the active phytoconstituents responsible for the activity and to carry out the *in-vivo* studies in order to elucidate the underlying mechanisms of action.

## ACKNOWLEDGEMENTS

Authors are thankful to President Dr. H. V. Dambal and Principal Dr. V. H. Kulkarni, SET's College of Pharmacy, S. R. Nagar, Dharwad for providing the facilities to carryout research work. Iwe are also thankful to CFC-SAIF-DST Centre Shivaji University, Kolhapur and MMCRL Belgaum for support and assistance in spectral analysis and *in-vitro* activities.

**Source of Support:** The author(s) received no financial support for the research, authorship, and/or publication of this article

**Conflict of Interest:** The author(s) declared no potential conflicts of interest with respect to the research, authorship, and/or publication of this article.

## REFERENCES

1. Mekky AE, Saied E, Al-Habibi MM, Shouaib ZA, Hasaballah AI, Rashed ME, et al. Eco- friendly biosynthesis of gold nanoparticles from *Amphimedon compressa* with antibacterial, antioxidant, anti-inflammatory, anti-biofilm, and insecticidal properties against disease vectors. Sci Rep. 2025;15(1):27845. doi:10.1038/s41598-025-11838-6. PMID:40738923 PMCID: PMC12311194

2. Patil TP, Vibhute AA, Patil SL, Dongale TD, Tiwari AP. Green synthesis of gold nanoparticles via *Capsicum annuum* fruit extract:

characterization, antiangiogenic, antioxidant and anti-inflammatory activities. Appl Surf Sci Adv. 2023;13:100372. doi:10.1016/j.apsadv.2023.100372.

3. Nkentsha Z, Rambharose S. Green-synthesized gold nanoparticles exhibit neuroprotective activity against oxidative stress-induced damage in SH-SY5Y cells. J Nanopart Res. 2025;27:197. doi:10.1007/s11051-025-06387-y.

4. Santhosh PB, Genova J, Chamati H. Green synthesis of gold nanoparticles: an eco- friendly approach. Chemistry. 2022;4(2):345-369. doi:10.3390/chemistry4020026.

5. Jaison JP, Balasubramanian B, Gangwar J, James N, Pappuswamy M, Anand AV, et al. Green synthesis of bioinspired nanoparticles mediated from plant extracts of Asteraceae family for potential biological applications. Antibiotics (Basel). 2023;12(3):543. doi:10.3390/antibiotics12030543. PMID: 36977506 PMCID: PMC10029979

6. Mehra V, Kumar S, Tamang AM, et al. Green synthesis of gold nanoparticles (AuNPs) by using plant extract and their biological application: a review. BioNanoSci. 2025;15:18. doi:10.1007/s12668-024-01703-7.

7. Evans WC, Trease GE. *Textbook of Pharmacognosy*. 15th ed. London: ELBS; 2002.

8. Iyengar MA. *Pharmacognosy Laboratory Manual*. Pune: Nirali Prakashan; 1998.

9. World Health Organization. *Quality Control Methods for Medicinal Plant Materials*. Geneva: World Health Organization; 1998.

10. Ayurvedic Pharmacopoeia Committee. *The Ayurvedic Pharmacopoeia of India*. New Delhi: Department of AYUSH, Ministry of Health and Family Welfare, Government of India; 2001. Vol 1, Pt 1:144-145.

11. Khandelwal KR. *Practical Pharmacognosy*. New Delhi: Pragati Books; 2008.

12. Kokate CK, Purohit AP, Gokhale SB. *Practical Pharmacognosy*. 2nd ed. Pune: Nirali Prakashan; 1994.

13. Belew AA, Hanan GGMW, Meshesha DS, Akele ML. Evaluation of total phenolic and flavonoid contents, antioxidant and antibacterial activity of leaf extracts from *Rhus vulgaris*. Discov Plants. 2025;2(1):141. doi:10.1007/s44372-025-00222-3.

14. Echeverry González SM, Santos AM, Júnior CCS, Saravanan S, Castellanos L, Serafini MR, et al. Natural therapies: a systematic review of the medicinal applications of *Passiflora ligularis*. Phytochem Rev. 2025;24:5685-5700. doi:10.1007/s11101-025-10087-9.

15. Hellany H, Badran A, Albahri G, Kafrouny N, El Kurdi R, Maresca M, et al. Biogenic synthesis of gold nanoparticles using *Scabiosa palaestina* extract: characterization, anticancer and antioxidant activities. Nanomaterials. 2025;15(17):1368. doi:10.3390/nano15171368. PMID: 39388278 PMCID: PMC11882267

16. Moosavy MH, de la Guardia M, Mokhtarzadeh A, Khatibi SA, Hosseinzadeh N, Hajipour N, et al. Green synthesis, characterization, and biological evaluation of gold and silver nanoparticles using *Mentha spicata* essential oil. Sci Rep. 2023;13(1):7230. doi:10.1038/s41598-023-33632-y. PMID: 37138528 PMCID: PMC10151037

17. Mardina V, Fadlly TA, Harmawan T, Sufriadi E, Iqramullah M, Umar H, et al. Green synthesis of gold nanoparticles from the aqueous extracts of *Sphagneticola trilobata* (L.) JF Pruski as anti-breast cancer agents. J Adv Pharm Technol Res. 2024;15(2):75-80. doi:10.4103/japtr.japtr_410_23. PMID: 38554828 PMCID: PMC11045784

18. Souza-Tarla CD, Uzuelli JA, Machado AA, Gerlach RF, Tanus-Santos JE. Methodological issues affecting the determination of plasma matrix metalloproteinase (MMP)-2 and MMP-9 activities. Clin Biochem. 2005;38(5):410-414.

doi: 10.1016/j.clinbiochem.2005.02.010. PMID: 15820487

19. Snoek-van Beurden PAM, Von den Hoff JW. Zymographic techniques for the analysis of matrix metalloproteinases and their inhibitors. Biotechniques. 2005;38(1):73-83. doi:10.2144/05381RV01. PMID: 15679089

20. Nandita R, Jeevitha M, Gurumoorthy K, Shanmugham R, Ravichandran S, Raj K. Anti- inflammatory activity and free radical scavenging activity of *Tridax procumbens* leaves- based chitosan gel. J Pharm Bioallied Sci. 2024;16(Suppl 4):S4081-S4084. doi:10.4103/jpbs.jpbs_1439_24.

21. Oselusi SO, Sibuyi NR, Meyer M, Madiehe AM. Anti-inflammatory, cytotoxic, and potential wound-healing effects of phytofabricated *Ehretia rigida* leaf aqueous extract- synthesized silver nanoparticles. Sci Rep. 2025;15(1):40301. doi:10.1038/s41598-025- 24111-7. PMID: 39996359 PMCID: PMC11990041

22. Patra JK, Das G, Fraceto LF, Campos EV, Rodriguez-Torres MD, Acosta-Torres LS, et al. Nano-based drug delivery systems: recent developments and future prospects. J Nanobiotechnol. 2018;16(1):71. doi:10.1186/s12951-018-0392-8. PMID: 30227815 PMCID: PMC6143217

23. Ahmed S, Ahmad M, Swami BL, Ikram S. A review on plant extract-mediated synthesis of silver nanoparticles for antimicrobial applications: a green expertise. J Adv Res. 2016;7(1):17-28. doi:10.1016/j.jare.2015.02.007. PMID: 26843967 PMCID: PMC4723742

24. Jara N, Milán NS, Rahman A, Mouheb L, Boffito DC, Jeffryes C, et al. Photochemical synthesis of gold and silver nanoparticles — a review. Molecules. 2021;26(15):4585. doi:10.3390/molecules26154585. PMID: 34362076 PMCID: PMC8347089

25. Farhana A, Alsrhani A, Nazam N, Ullah MI, Khan YS, Rasheed Z. Gold nanoparticles inhibit PMA-induced MMP-9 expression via microRNA-204-5p upregulation and deactivation of NF-κB p65 in breast cancer cells. Biology. 2023;12(6):777. doi:10.3390/biology12060777. PMID: 37374496 PMCID: PMC1030608

26. Sowndarya A, Thangadurai TD, Thomas NG, Sreedharan R, Anil S, Manjubaashini N, et al. Effect of surface-engineered AuNPs on gene expression, bacterial interaction, protein denaturation, and toxicology assay: an in vitro and in vivo model. J Mater Chem B. 2025;13(7):2409-2417. doi:10.1039/D4TB01731E.